



## Technical note: Pleistocene climate sensitivity to CO<sub>2</sub> forcing is path dependent in reconstructions

Roger M. Cooke<sup>1</sup>, Willy P. Aspinall<sup>2</sup>

<sup>1</sup>Resources for the Future, Washington DC, 200036 USA

5 <sup>2</sup> School of Earth Sciences, University of Bristol, Bristol, UK

Correspondence to: Roger M. Cooke (cooke@rff.org)

**Abstract.** Improved high-resolution paleo records of atmospheric carbon dioxide (CO<sub>2</sub>) concentrations and reconstructions of Earth's surface temperature are available. We analyse one authoritative Pleistocene dataset to explore how the climate sensitivity parameter  $S$  varies under different system states, using linear regression of mean annual surface temperature changes against CO<sub>2</sub> forcing changes. Data are partitioned by *path* (deglaciation or glaciation). On the whole data set,  $S = 2.04\text{K/Wm}^{-2}$  and CO<sub>2</sub> forcing explains 64% of the variance in temperature. During deglaciation periods,  $S = 2.34\text{K/Wm}^{-2}$ , explaining 75% of the temperature variance.; during glaciations,  $S = 1.59\text{K/Wm}^{-2}$  and explains 48% of the temperature variance. Possible process-related explanations for these *path*-related differences are conjectured.

### 15 1 Introduction

The climate sensitivity parameter  $S$  is somewhat loosely defined in the literature (Myhre et al 2013) as the change with respect to present in mean annual global surface temperature ( $\Delta T$ ) per unit change in forcing with respect to present ( $\Delta F$ ).  $S$  is sometimes estimated from data by linear regression:  $\Delta T = S \times \Delta F + B + e$  with intercept  $B$  and error  $e$ .  $\Delta F$  is [ $\text{Wm}^{-2}$ ] so that  $S$  is [ $\text{K}/(\text{Wm}^{-2})$ ]. The variance of  $e$  is estimated as  $(SS - SSR)/(N - df - 1)$  where  $N$  is the number of observations,  $df$  is the number of parameters in the model (here always =1),  $SS$  is the sum square deviations from the population mean and  $SSR$  is the sum square deviations of the regression estimates from the population mean.  $SSR/SS$  is the fraction of variance of  $\Delta T$  explained by the regression model, termed  $R^2$ . The lower is  $R^2$  the more of the variation in  $\Delta T$  must be attributed to factors other than  $\Delta F$ .

25 It is widely believed that "... the change in surface temperature is directly proportional to the radiative forcing. Hence, this becomes the simplest way of quantifying the effect in a perturbation in greenhouse gas inventory" (Byrne and Goldblatt 2014). Note that  $\Delta T$  can be proportional to  $\Delta F$  only if the intercept  $B$  is zero. Assuming  $B = 0$  forces the trend line to pass through the origin ( $\Delta F = 0, \Delta T = 0$ ). This can inflate and skew the errors and can cause the regression model to be a worse predictor of the data than simply predicting the mean of  $\Delta T$  for each value of  $\Delta F$  (as happens here, see Figure 1 and



30 associated discussion). Others argue that the regression line “needs to pass through the origin to avoid any biases” (Köhler et al 2017). Different statistical packages have different interpretations of  $R^2$  when  $B = 0$  is stipulated, but none has the interpretation as fraction of explained variance (see SI), thereby disabling this important diagnostic. In what follows, we refrain from stating  $R^2$  values if  $B$  is set to zero. Of course, the placement of the origin effects the value of  $S$  if  $B = 0$  is stipulated. For example, Snyder (2019) considers  $\Delta T$  relative to the average temperature over the last five thousand years, 35 whereas Martínez-Boti et al (2015) define temperature change relative to pre-industrial temperature. If the intercept is estimated this choice is immaterial. In any event, the consequences of stipulating  $B = 0$  are large and should be carefully weighed.

Here, we utilize the dataset (Martínez-Boti et al 2015) for the Pleistocene (1096 records from 0.14 to 798.51 kaBP (thousand 40 years before present). A second Pleistocene dataset (Snyder, 2019) yields very similar results and is discussed briefly. In recent years, several researchers have studied paleoclimate data for evidence of “state dependence” in the climate sensitivity parameter (e.g. Meraner et al 2013). It has been observed that the linear approximation breaks down in the long tail of high climate sensitivity commonly seen in observational studies (Bloch-Johnson et al 2015). Transient behavior of climate sensitivity has been explored using an energy balance model combined with observational and modeling CMIP5 constraints 45 (Goodwin, 2018). Background state dependence and tipping points in Earth system sensitivity with millennial timescales (von der Heydt et al 2016) motivate the introduction of the more general “climate sensitivity parameter”. Others find that climate sensitivity strongly depends on the climate background state, with significantly larger values attained during warm phases (Meraner et al 2013, Friedrich et al 2016). Some authors voice concerns over the simple concepts underlying climate sensitivity and radiative forcing (Knutti et al 2010). Non-linear dependence of land ice albedo forcing is found (Köhler et al 50 2010), while non-linearity of  $CO_2$  forcing is said to depend on the  $CO_2$  data set. Global mean temperature and  $CO_2$  diverge during intervals of pronounced land ice growth (Köhler et al 2018). The need to distinguish actuo- and paleoclimate sensitivity over different time scales is emphasized (Rohling et al 2018). Averaged glacial and interglacial climate sensitivities are estimated (Shao et al 2019) using Earth system model simulations of the Last Glacial Cycle.

55 The present study applies standard regression analysis to study variations in the climate sensitivity parameter, using Pleistocene data from Martínez-Boti et al (2015). Rather than estimating non-linear regression functions, we partition the data into periods of increasing versus periods of decreasing paths of  $CO_2$  concentration corresponding to deglaciation versus glaciation respectively. The SI also looks at partitions into epochs before and after 424 kaBP and periods of low, intermediate and high  $CO_2$  concentration. The path dependence is the most important followed by epochal dependence. 60 Dependence on background  $CO_2$  concentration has low explanatory power but does interact with the other two (see SI).

To compute the fraction of explained variance it is necessary to estimate the intercept term. Comparison with regressions in which the intercept  $B$  is set to zero shows that the latter have higher values of the climate sensitivity parameter with much



less variation over the partition elements. While this data may be subject to errors, random errors would depress the  $R^2$   
65 values. The wide variation of  $R^2$  values across the partition elements argues against a strong random or systematic error  
across the entire data set.

Given the wide variations in  $S$ , projections of regression equations to estimate  $CO_2$  concentrations out of sample cannot be  
considered predictions unless the conditions going forward are very similar to the conditions on which such regressions are  
70 based.

## 2. Analysis of Pleistocene data

A deterministic functional relation between changes in  $CO_2$  concentrations and changes in the induced forcing ( $\Delta FCO_2$ ) is  
75 inferred from radiative transfer codes, where 278 ppmv is taken as the pre-industrial concentration of  $CO_2$ :

$$\Delta FCO_2 (CO_2) = 5.3515 \times \ln(CO_2/278) [Wm^{-2}]. \quad (1)$$

Note that the forcing change depends only on the ratio of two  $CO_2$  concentrations and not on their actual values. This  
80 assumption is pervasive in the literature. Doubling  $CO_2$  with respect to pre-industrial:

$$\Delta FCO_2 (556) = 3.71 [Wm^{-2}]. \quad (2)$$

Regressing mean annual surface temperature ( $\Delta MAT$  in Martinez-Boti et al 2015) on  $\Delta FCO_2$  gives the following equation  
85 which explains 64% of the variance in  $\Delta T$ :

$$\Delta T(\Delta FCO_2) = 2.037 \times \Delta FCO_2 - 0.709 + e \quad (3)$$

The climate sensitivity parameter  $S = 2.037 [K/Wm^{-2}]$ . The values of  $S$  and  $B$  in eqn. (3) are chosen to minimize the squared  
90 distance between the values of  $\Delta T$  and the linear trend.

To project the effect on temperature of doubling  $CO_2$  above pre-industrial, based on the whole Pleistocene data, substitute  
 $\Delta FCO_2 = 3.71$  in (3) and find  $\Delta T(556) = +6.85^\circ K$ . Neglecting the intercept term would result in:  $2.037 [K/Wm^{-2}] \times 3.71 [W]$



=  $+7.56^{\circ}\text{K}$ . This, of course, is incorrect: if we wish to constrain the intercept to be zero, we must find the line passing  
95 through the origin minimizing squared distance to  $\Delta T$ . In that case,  $S = 2.531\text{K/Wm}^{-2}$ ,  $\Delta T(556) = +9.391^{\circ}\text{K}$  (Figure 1).

Eqn. (1) is just a positive affine transformation of  $\ln(\text{CO}_2)$ . If we regress  $\Delta T$  on  $\ln(\text{CO}_2)$ , we would also explain 64% of the  
variance and also find  $\Delta T(556) = +6.85^{\circ}\text{K}$ . The only difference would be that the units of the linear coefficient would be  
[ $\text{K}/\ln(\text{ppmv})$ ], instead of [ $\text{K/Wm}^{-2}$ ]. The latter dimension suggests physical agency; indeed, a *GHG* induced radiative  
100 imbalance at the top of the atmosphere causes warming according to the Stefan Boltzmann law. At the same time, a rise in  
temperature can raise atmospheric  $\text{CO}_2$  concentrations through temperature mediated feedbacks as, for example, when higher  
ocean temperatures reduce  $\text{CO}_2$  uptake in the oceans. We retain the familiar dimension of  $\text{K/Wm}^{-2}$  for the climate sensitivity  
parameter while recognizing that it reflects a choice of units rather than physical agency.

105 For the Pleistocene data of Martinez-Boti et al (2015), the mean  $\Delta T = -2.816^{\circ}\text{K}$ . Letting  $i$  index the 1096 data points,  
summing the squared deviations from the mean of the black regression line ( $B = 0$ ) in Figure 1 left gives  $\text{SSR} = \sum_i (2.531 \times$   
 $\Delta \text{FCO}_2(i) + 2.816)^2 = 2969 > 2942 = \sum_i (\Delta T(i) + 2.816)^2 = \text{SS}$ . Using the black line as a predictor of  $\Delta T$  is a bit worse than  
predicting the population mean of  $\Delta T$  for each value of  $\Delta \text{FCO}_2(i)$ . For the red regression line ( $B$  estimated),  $\text{SSR} = \sum_i$   
 $(2.037 \times \Delta \text{FCO}_2(i) - 0.709 + 2.816)^2 = 1896$ , which explains  $1896/2942 = 0.644$  (64%) of the variance of  $\Delta T$ .

110

Neglecting to clarify whether the intercept is inferred or stipulated invites confusion. In this data, setting  $B = 0$  inflates the  $S$   
values and suppresses the differences over different partition elements. Table 1 compares results with and without the  
intercept assumption.

## 115 2. Partitioning the data

Figure 2 shows  $\text{CO}_2$  as a function of age in *kaBP*, with local minima and maxima identified with blue *resp* red arrows. This  
enables us to distinguish episodes of increasing (deglaciation) and decreasing (glaciation)  $\text{CO}_2$  concentrations. Note that  
increasing  $\text{CO}_2$  episodes generally transpire more quickly than decreasing  $\text{CO}_2$  episodes. Dividing the data into two subsets  
consisting of increasing or decreasing episodes allows us to determine whether the climate sensitivity parameter is  $\text{CO}_2$  -  
120 path dependent. Figure 2 also suggests that the Earth's climate system changed around the inception of Marine Isotope  
Stage 11 in 424 *kaBP*, midway between a glacial maximum and a glacial minimum. The SI examines epochal dependence by  
comparing sensitivity in the periods before and after 424 *kaBP* and the results are in Table 1.



125 The results show evidence of path dependence. Note that if the intercept is estimated the differences in the climate sensitivity  
parameter between glaciation and deglaciation (1.5885, 2.3352) are larger than if the intercept is stipulated to be zero  
(2.5051, 2.552). The same is true for the projected temperature at 522ppmv  $CO_2$ : with the intercept estimated these are  
(4.72, 8.32) but with intercept stipulated these are (9.16, 9.47). The right panel of Figure 2 showing glaciation also  
illustrates how stipulating the intercept can lead to inferior predictions. Summing over the 583 data points in the right panel,  
the square differences between  $\Delta T$  and the prediction with intercept = 0 (red line) is 674.1, whereas when the intercept is  
130 estimated this sum is (blue line) 478.7. Note also the difference in explanatory power in the two panels. During deglaciation  
the blue regression line explains three fourths of the variance in  $\Delta T$  whereas during glaciation less than half of the variance is  
explained. The interpretation is that during glaciation factors other than  $CO_2$  account for the variation in  $\Delta T$ .

A more recent study (Snyder 2019) presents a Pleistocene data set that contains 799 records, evenly spaced in steps of  
135 1000yr. Modeling, subjective probabilities and Monte Carlo analysis are applied in Snyder (2019) to quantify uncertainties  
in data and variable relationships. Changes in temperature with respect to the average over the last 5000 years are regressed  
on the total change in forcing ( $\Delta R$ ) from Green House Gases, Land Ice, dust and vegetation. A good comparison with  
Martinez-Boti et al (2015) is obtained by considering just the medians of the various terms. With respect to Snyder (2019)  
data, regressing the median of  $\Delta T$  (termed Global Annual Surface Temperature GAST) on the median of  $\Delta FGHG$ , with  
140 intercept, yields:

$$\Delta T(\Delta FGHG) = 1.962 \times \Delta FGHG - 0.788 + e; \Delta T(556) = +6.49K$$

which compares well with eqn. (3), above, especially if we consider that Snyder (2019) estimates change in temperature with  
145 respect to the average surface temperature over the last 5000 years which, according to Martinez-Boti et al (2015), is 0.45K  
higher than the pre-industrial reference value in their analysis. Hence we should compare  $6.49 + 0.45 = +6.94K$  to  $+6.85K$   
from eqn. (3). The medians of the separate forcing terms  $\Delta R_{[GHG]}$ ,  $\Delta R_{[LI]}$ ,  $\Delta R_{[AE]}$ ,  $\Delta R_{[VG]}$  are all highly correlated with each  
other and with  $\Delta T$ . Separating these forcing contributions means assuring that, on 1000yr timescales, land ice, dust and  
vegetation forcings are not already bleeding into the GHG forcing. This issue is avoided by focusing just on GHG forcing.  
150 The penalty is that conclusions are wedded to the 1000yr timescale.

Summary statistics comparing results with and without  $B = 0$  are presented in Table 1: the partitions Pre and Post 424 kaBP  
are intersected with deglaciation and glaciation periods.



155 **Summary and discussion**

Extending previous analyses of Pleistocene climate data of Martinez-Boti et al (2015) and Snyder (2019), one key finding is that imposing a zero intercept tends to mask differences between the climate sensitivity parameter in different subsets of the Pleistocene data. This assumption produces inferior predictions relative to regressions in which estimates of intercept are exploited. Ultimately, this prevents us from appreciating the role of explanatory power in comparing the climate sensitivity parameter in different physical situations.

Explaining why the climate sensitivity parameter is higher during deglaciation than during glaciation is a challenge which deserves attention. One obvious feature is the fact that deglaciation generally transpires faster than glaciation. It may be that certain negative feedbacks with intermediate time scales are allowed to play out during glaciation but are less effective during rapid deglaciation. For example, carbon fertilization would draw down atmospheric  $CO_2$ . During glaciation the retreat of plants would tend to retard the cooling and slow the glaciation process. During deglaciation the advance of plants would tend to retard the warming process. However, if the retreat of land and sea ice happened quickly, other changes such as growth of the Hadley cells and desertification might overwhelm the advance of plants and disable this negative feedback. Oceanic  $CO_2$  outgassing during the last deglaciation has been proposed (Shao et al 2019) as a potential disequilibrium process influencing atmospheric  $CO_2$  concentrations. Aerosols, and glacial aerosols specifically, can interact with clouds and influence radiative forcing; paleo-aerosol concentrations are likely to have varied with glaciation pathways. However, the lack of robust reconstructions of glacial aerosol forcing is a key source of uncertainty in paleo-based estimates of climate sensitivity (Friedrich, and Timmermann, 2020). As a further possibility, Xie (2020) posits that non-uniform regional uptake of heat by oceans militates against equilibration with radiative forcing, with spatio-temporal variations in ocean state and currents affecting global climate sensitivity.

These are some conceptual examples of how the interplay of process-related feedbacks with different time scales might alter climate sensitivity in different physical situations. The supplementary material shows that the climate sensitivity parameter is higher after *424KaBP*, than before. Such effects have been attributed to changes in orbital forcing, though a detailed understanding of why heightened forcing raises climate sensitivity has not, to our knowledge, been found.

If the Earth's surface temperature response to  $CO_2$  forcing on millennial time scales does indeed depend on the physical circumstances at the time of the forcing, predictions for the Earth's future response to heightened  $CO_2$  forcing require knowledge of these complex non-linear interactions, understanding how they will evolve and on what timescales. Scrutiny and clarification of assumptions regarding the intercept issue and further analytical investigation with stochastic uncertainty techniques should provide additional insights into the properties of the climate sensitivity parameter and inform discussion of contingent implications.



**Acknowledgments** The authors are grateful to Gavin Foster and Tom Gernon for subject matter advice, and to Gordon Woo for commenting on a draft manuscript.

190

#### References

- Bloch-Johnson, J., Pierrehumbert, R. T. & Abbot, D. S. Feedback temperature dependence determines the risk of high warming. *Geophys. Res. Lett.* 42, 4973–4980, doi:10.1002/2015GL06424 (2015).
- Byrne, B. & Goldblatt, C. Radiative forcing at high concentrations of well-mixed greenhouse gases. *Geophys. Res. Lett.* 41, 152–160, doi:10.1002/2013GL058456 (2014).
- Friedrich, T. & Timmermann, A. Using Late Pleistocene sea surface temperature reconstructions to constrain future greenhouse warming. *Earth Planet. Sci. Lett.* 530, 115911 doi: 10.1016/j.epsl.2019.115911 (2020).
- Friedrich, T. et al. Nonlinear climate sensitivity and its implications for future greenhouse warming. *Sci. Adv.* 2, e1501923 (2016).
- 200 Goodwin, P. On the time evolution of climate sensitivity and future warming. *Earth's Future* 6, 1336–1348, doi:10.1029/2018EF000889 (2018),
- Knutti, R., Rugenstein, M. A. A. & Hegerl, G. C. Beyond equilibrium climate sensitivity. *Nature Geoscience* 10, 727–736; doi: 10.1038/NNGEO3017 (2017).
- Köhler, P. et al. A state-dependent quantification of climate sensitivity based on paleodata of the last 2.1 million years. *Paleoceanography* 32, 1102–1114; <https://doi.org/10.1002/2017PA003190> (2017).
- 205 Köhler, P. et al. The effect of obliquity-driven changes on paleoclimate sensitivity during the late Pleistocene. *Geophys. Res. Lett.* 45, 6661–6671; doi:10.1029/2018GL077717 (2018).
- Köhler, P. et al. What caused Earth's temperature variations during the last 800,000 years? Data-based evidence on radiative forcing and constraints on climate sensitivity. *Quat. Sci. Rev.* 29, 129–145; 9-145 doi: 10.1016/j.quascirev.2009.09.026 (2010).
- 210 Martínez-Botí, M. A. et al. Plio-Pleistocene climate sensitivity evaluated using high-resolution CO<sub>2</sub> records. *Nature* 518, 49–54; doi:10.1038/nature14145 (2015).
- Meraner, K., Mauritsen, T. & Voigt, A. Robust increase in equilibrium climate sensitivity under global warming. *Geophys. Res. Lett.* 40, 5944–5948; doi:10.1002/2013GL058118 (2013).
- 215 Myhre, G. et al. Anthropogenic and Natural Radiative Forcing Supplementary Material. In: *Climate Change 2013: The Physical Science Basis. Contribution of Working Group I to the Fifth Assessment Report of the Intergovernmental Panel on Climate Change* [Stocker, T.F. et al. (eds.)]. Available from [www.climatechange2013.org](http://www.climatechange2013.org) and [www.ipcc.ch](http://www.ipcc.ch) (2013).
- Rohling, E.J. et al. Comparing Climate Sensitivity, Past and Present. *Annu. Rev. Mar. Sci.* 10:12.1–12.28. doi:10.1146/annurev-marine-121916-063242 (2018).
- 220 Shao, J. et al. Atmosphere-Ocean CO<sub>2</sub> Exchange Across the Last Deglaciation from the Boron Isotope Proxy. *Paleoceanography and Paleoclimatology* 34, 1650–1670, doi:10.1029/2018pa003498 (2019).



- Shao, J. et al. Atmosphere-Ocean CO<sub>2</sub> Exchange Across the Last Deglaciation from the Boron Isotope Proxy. *Paleoceanography and Paleoclimatology* 34, 1650-1670, doi:10.1029/2018pa003498 (2019).
- Snyder, C.W. Revised estimates of paleoclimate sensitivity over the past 800,000 years. *Climatic Change* 156, 121-138; doi:10.1007/s10584-019-02536-0 (2019).
- 225
- Von der Heydt, A.S. et al. Lessons on Climate Sensitivity from Past Climate Changes. *Curr. Clim. Change Rep.* 2, 148-158; doi: 10.1007/s40641-016-0049-3 (2016).
- Xie, S.-P. Ocean Warming Pattern Effect on Global and Regional Climate Change. *AGU Advances* 1, e2019AV000130, doi:10.1029/2019av000130 (2020).
- 230

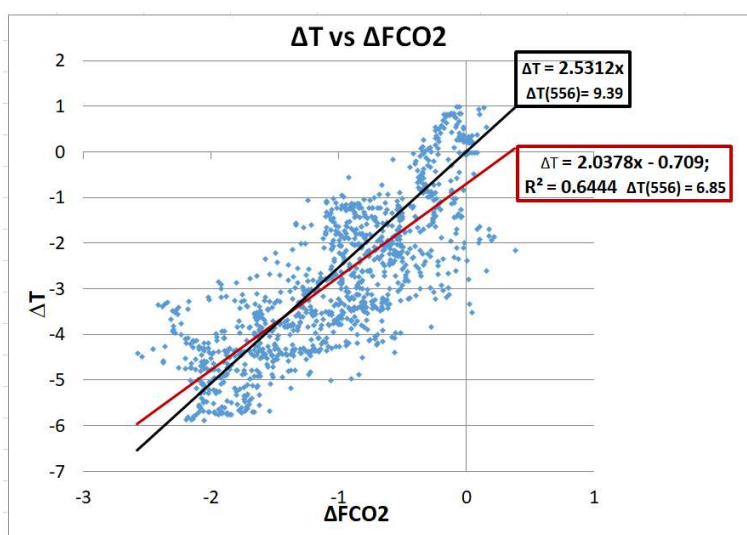
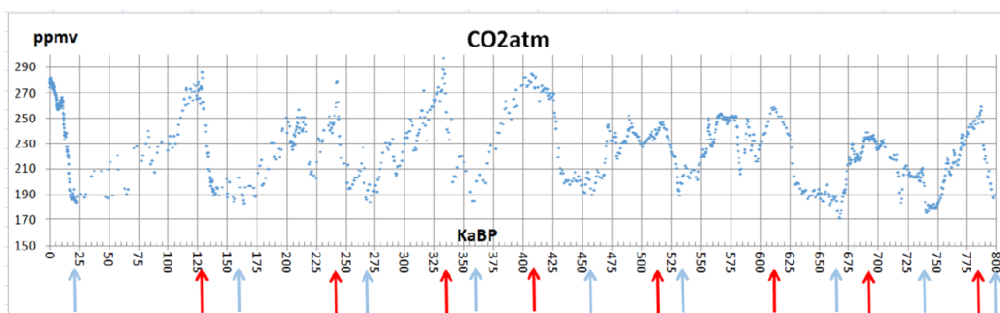


Figure 1: Regression of  $\Delta T$  on  $\Delta FCO_2$  for all Pleistocene data; with (red) and without (black) intercept. Out of sample values for doubling pre-industrial CO<sub>2</sub>,  $\Delta T(556)$  are also shown.







235 Figure 2: CO<sub>2</sub> concentrations as function of kaBP. Blue arrows indicate local minima, red arrows indicate local maxima.

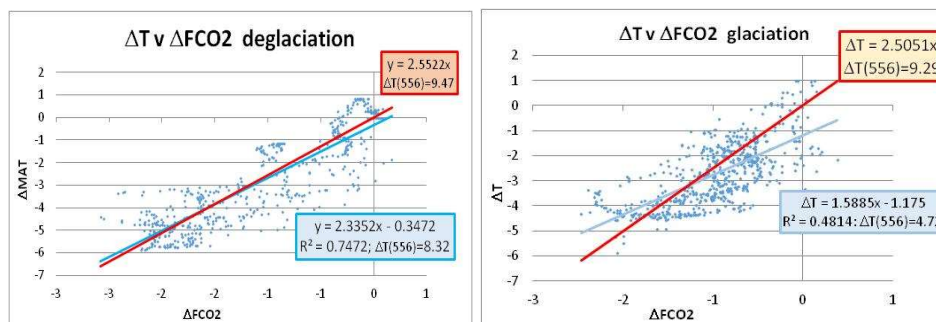


Figure 3: Deglaciation, (left, increasing) and glaciation (right, decreasing) CO<sub>2</sub> paths. Regression for B=0 stipulated in Red, with B estimated in Blue.

240

	Intercept estimated					Intercept stipulated = 0		
	R <sup>2</sup>	S	B	SE	ΔT(556)	S	SE	ΔT(556)
All (1096)	0.644	2.038	-0.709	0.978	6.851	2.531	1.047	9.391
ALL Pre 424 (546)	0.419	1.427	-1.535	0.883	3.760	2.489	1.082	9.232
All Post 424 (550)	0.726	2.320	-0.395	0.994	8.212	2.595	1.006	9.626
De-Glaciation (increasing CO <sub>2</sub> )								
All (513)	0.747	2.333	-0.348	0.996	8.309	2.552	1.014	9.469
Pre 424 (220)	0.457	1.804	-0.959	1.009	5.733	2.420	1.145	8.977
Post 424 (293)	0.830	2.631	-0.215	0.916	9.545	2.798	0.781	10.381
Glaciation (decreasing CO <sub>2</sub> )								
All (583)	0.481	1.588	-1.175	0.908	4.718	2.505	1.076	9.294
Pre 424 (326)	0.352	1.170	-1.833	0.759	2.507	2.593	1.061	9.621
post 424 (257)	0.538	1.744	-0.782	0.980	5.689	2.359	1.080	8.752
Low, Medium, High CO <sub>2</sub>								
<210 (305)	0.022	0.485	-3.576	0.779	-1.778	2.367	0.902	8.781
210...250 (493)	0.195	1.913	-0.943	0.953	6.156	2.810	0.978	10.424
>250 (298)	0.201	2.711	-0.396	1.096	9.664	3.670	1.123	13.614

Table 1: Summary of data subset regressions. R<sup>2</sup> is the fraction of variance of ΔT explained by the regression, S is the climate sensitivity parameter, B is the intercept, SE is the standard deviation of the difference between predictions and true values, and ΔT(556) is the projected ΔT corresponding to a doubling of the pre-industrial CO<sub>2</sub> concentration (278 ppmv). With the exception



245 of “All” and “Pre 424” all S values are outside the 90% confidence bands of the other values within each group. The number of samples is in parentheses.